Single-Step Thermal Method to Measure Intracrystalline Mass Diffusion in Adsorbents

Ph. Grenier, V. Bourdin, L. M. Sun, and F. Meunier
LIMSI BP 133 91403 Orsay, France

A single-step thermal method is used to measure intracrystalline mass diffusion. Sorption/desorption rates in zeolite samples (large crystals, monolayers of pellets, or even a single pellet) after a pressure or volume step are followed by monitoring the sample surface temperature by infrared detection. For a volume step, the pressure is also measured yielding the adsorbed mass. Sorption rates of water vapor in NaX are measured both on large 100-μm crystals and pellets. This fast system corresponds to the limit of the pressure-step thermal method (using 100-μm crystals). Sorption rates of methanol in the same large NaX crystals show good precision by the pressure-step method. The methanol results show that a surface barrier may occur after thermal regeneration of the sample in the presence of methanol traces. A major advantage of this method is that the shape of response curves can provide useful information on the nature of the mass-transfer resistance despite its limits. Sorption rates of methanol vapor on mordenite H (zeolon) pellets prove that the intracrystalline diffusivity may be extracted from pellet measurements for a slow diffusing species.

Introduction

The intracrystalline diffusion coefficient of a single gas component species in zeolites may vary from 10^{-8} m^2s^{-1} for fast diffusing species down to 10^{-22} m^2s^{-1} or less for slow diffusing species, depending on steric effects as well as on molecular interactions between adsorbed molecules and the adsorbent framework (Kärger and Ruthven, 1989). Equilibrium molecular dynamics simulations have been performed on a number of sorbate–zeolite systems to obtain the diffusivity but, at the moment, the prediction of diffusivity is only possible for simple spherical molecules in simple framework structures (Smivoc et al., 1991; Maginn et al., 1992).

The precise experimental measurement of intracrystalline diffusion coefficients is important for two main reasons:

- To better understand the diffusion mechanisms inside the micropores
- To provide a tool for precise determination of the limiting effects during heat and mass transfer in adsorbers.

Following Kärger and Ruthven (1992), the intracrystalline diffusion coefficients can be measured by either microscopic techniques [such as NMR (Pfeifer, 1976) and neutron scattering (Jobic et al., 1989)] or macroscopic techniques [such as uptake rate measurements (Barrer and Brook, 1953; Beschmann et al., 1990), chromatography (Schneider and Smith, 1968; Ruthven and Kumar, 1980; Chiang et al., 1984), permeation (Hayhurst and Paravar, 1988), frequency response (Yasuda et al., 1991; Van den Begin and Rees, 1989), and zero length column (Eic and Ruthven, 1988)]. The microscopic techniques investigate the system under thermodynamic equilibrium and yield the self-diffusivity, which is calculated by the Einstein relation.

In the macroscopic techniques, a concentration gradient exists. The quantity obtained is the intracrystalline transport diffusivity defined according to the Fick's first law as

$$J = -D_c \nabla q, \tag{1}$$

where J is the flux and q is the sorbate concentration.

Although the physical effects that govern these two phenomena are distinct, the Fickian transport diffusivity and the self-diffusivity are strictly equal in the low concentration limit (Kärger and Ruthven, 1992). At finite concentrations, it is generally stated that the self and the corrected Fickian transport diffusivities are nearly equal (Kärger and Ruthven, 1992). The corrected Fickian diffusivity is defined as

$$D_0 = D_c \left(\frac{\partial \ln q}{\partial \ln p} \right)_T, \tag{2}$$

where p is the pressure of the adsorbate in the gas phase, q is the equilibrium adsorbed phase concentration, and D_0 is the corrected Fickian diffusivity.

Comparisons between self-diffusivity and transport diffusivity are possible only for a limited range of experimental systems. This is because microscopic techniques work best for diffusivities in the range 10^{-8}–10^{-12} $m^2 \cdot s^{-1}$, whereas it is difficult to obtain reliable macroscopic data when the diffusivity is greater than about 10^{-11} $m^2 \cdot s^{-1}$ with currently available macroscopic techniques. Satisfactory agreement is observed between the macroscopic and microscopic measurements for several systems. Nevertheless, large experimental discrepancies are still being reported (Kärger and Ruthven, 1989). Generally, the intraparticle diffusion coefficient as measured by microscopic techniques is high when a discrepancy exists. The origin of these discrepancies remains unclear.

There is a need to measure with precision intracrystalline diffusivities with macroscopic techniques since adsorptive processes always deal with mass transfer under concentration gradients. Engineers need reliable data for adsorption diffusivities as well as for adsorption equilibrium to be able to correctly design adsorbers. The precise determination of the intracrystalline diffusivity through macroscopic techniques is a real problem, mostly for fast-diffusing species. Sophisticated techniques are required to measure those coefficients with a good precision. First of all, a reliable technique must be free from artifacts that may be responsible for misinterpretations of the experimental results. Two artifacts are now well known (Kärger and Ruthven, 1992):

- Heat effects can be very important in uptake experiments when there is no carrier gas; this can lead to large errors when isothermal models are used.
- "Bed" effects due to the propagation of the pressure wave in a shallow bed during a single-step uptake experiment can lead to an extraneous mass-transfer limitation (Zhong et al., 1993).

These effects add an extraneous transfer limitation, and thus the unwary investigator may conclude that the mass-transfer resistance is substantially larger than it actually is. This explains why some results were interpreted as mass diffusion limitations in the past while they were more likely caused by other effects.

The aim of this article is to present a novel experimental technique that is based on the surface sample infrared (IR) temperature measurement. In parallel with the experimental technique, a detailed nonisothermal heat- and mass-transfer model is developed for the analysis of the experimental results (Sun and Meunier, 1987a). To demonstrate the validity of the technique, results obtained on specially grown large crystals are presented first. As one of the advantages of this technique is to provide an opportunity to extract intracrystalline diffusion coefficients from industrial pellets, examples of the extraction of such data from pellets are also presented.

Experimental

Experimental equipment

Three techniques were successively used at LIMSI to measure the kinetics of adsorption: pressure step, volume step, and frequency response. Only the first two techniques will be presented here; the frequency response experiments are under analysis and will be reported in the future. The main originality of the equipment built at LIMSI (Figure 1) is the use of an IR detector for measuring the zeolite surface temperature (Torresan and Grenier, 1992). It differs from the method proposed recently by Karge and Niessen (1991), which uses FTIR measurements to monitor the adsorbed phase concentration. In the system described herein, the IR technique is used to monitor the sample surface temperature. Although it is a thermal signal, it is also a measure of mass diffusion because adsorption is strongly exothermic and mass transfer is always associated with heat generation in an uptake experiment. The major advantages of this technique are:

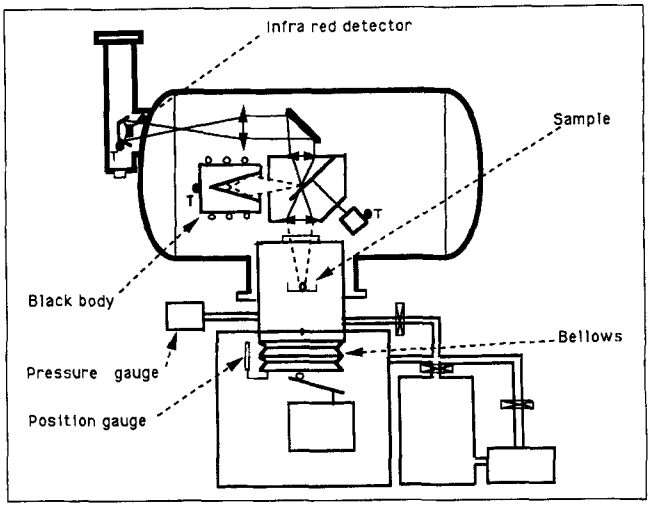

Figure 1. Experimental equipment.

- No intrusive perturbations (no sensor) during the experiment
- High temperature sensitivity ($\sim 10^{-3}$°C)
- Short response time constant ($\sim 10^{-3}$ s)
- Possibility to precisely focus the temperature measurement on a small region enabling the measurement of a single-pellet response.

Besides the high precision of the surface temperature measurement, attempts have been devoted to measuring simultaneously and with similar precision the adsorbed mass as a function of time. A piezometric method gives the adsorbed mass through a precise and rapid response pressure sensor (Baratron) when a volume-step technique is used. This technique is found to be very reliable as long as the sample mass is large enough (this point is discussed later). If the sample mass is too small, less than about 0.1 g (which is usually the case for a single layer of crystals), the mass of adsorbate cannot be measured with precision; only the temperature response is experimentally available.

Experimental procedure

Pressure step. The sample is placed on a very thin (10 μm) stainless-steel sheet inside a chamber of known volume (1.2 L). This changer is connected through a solenoid valve to a much larger buffer vessel (105 L) so that opening of the

solenoid valve gives a rapid change in pressure. The IR emission from the sample is measured by a HgCdTe photoconductive detector. The detector gives an output signal, by means of a chopper and lock-in amplifier, proportional to the temperature difference between the sample and a thermostatically controlled black body.

Starting from an initial pressure of P_0 and temperature T_0, the sample is subjected to a positive or a negative pressure step. The large buffer vessel ensures that the quantity of sorbate adsorbed by the sample is small relative to the total quantity of sorbate in the system. Thus, after the pressure step, the pressure remains constant. The IR emission and the pressure are monitored 12 times per second during the first few seconds. Sampling is continued at a lower rate until thermal equilibrium is reached ($T - T_0 < 0.02$ K).

Volume step. The experimental protocol is the same as in the case of the pressure step except that the pressure step is produced by a sudden compression of a bellows and the buffer vessel is not used. In this version of the equipment, the chamber volume was only 0.6 L. The first advantage of the volume-step protocol is that the total mass of the adsorbate (gas + adsorbed phase) is constant during the experiment. Therefore, a very precise and rapid piezometric mass determination is possible provided the pressure is monitored with precision. This information is not available from the pressure-step protocol. The second advantage of this protocol is that since the pressure variation is faster than with a pressure-step, the precision is better for fast-diffusing species.

Model. The nonisothermal kinetics of an adsorbent particle [crystal (Ruthven, 1984) or a bidispersed particle (Sun and Meunier, 1987a)], which is subjected at time zero to a change in the surrounding adsorbate pressure, is defined by a set of differential equations for diffusion and heat transfer in the particle that can be solved numerically (see appendix).

Experimental results. Two cases will be presented to illustrate the methodology for extraction of the intracrystalline coefficient of diffusion; specially grown large crystals and standard industrial pellets.

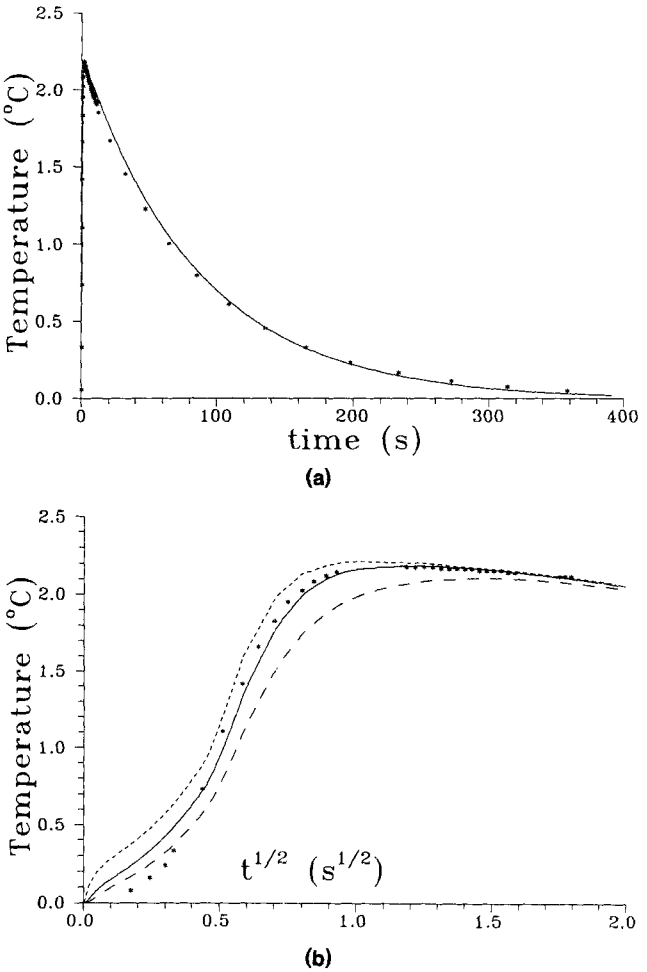

Figure 2. Temperature response of a 100-μm NaX crystals single layer after a pressure step of H_2O vapor (see Table 1).

(a) Experimental measurements (symbols) and best theoretical fit (solid line). (b) Influence of the intracrystalline diffusion coefficient at short times (full line, $D_0 = 0.6\ 10^{-10}$ $m^2 \cdot s^{-1}$; short dashes, $D_0 = 6\ 10^{-10}$ $m^2 \cdot s^{-1}$; long dashes, $D_0 = 0.2\ 10^{-10}$ $m^2 \cdot s^{-1}$).

Large crystals (pressure step)

Large 100-μm NaX crystals synthesized by Zhdanov have been used in this study.

NaX–H_2O (100-μm crystals). A typical experimental run is shown in Figure 2, in the case of a positive-pressure step. After the pressure step, a sharp temperature peak is observed; it corresponds to the heat generated during the adsorption process. The physical phenomena can be analyzed in three stages.

1. At the very beginning, immediately after the pressure step, quasi-adiabatic adsorption occurs. Heat generation through adsorption is much more important than heat exchange with the environment during this stage. According to Eq. A4, temperature and mass variations are proportional as long as the term $[(\sigma + 1)h/R_c](T - T_0)$ is small in comparison to the other terms of Eq. A4. The adsorption rate is thus governed by mass diffusion as long as the sample temperature variation is small.

2. The sample temperature increases as adsorption proceeds. The contribution of the term $[(\sigma + 1)h/R_c](T - T_0)$ in Eq. A4 increases and tends to slow down the temperature increase. When the heat generated by adsorption and the heat exchange with the environment are equal and opposite, Eq. A4 leads to $(dT/dt) = 0$; the temperature reaches a maximum. Both mass diffusion and heat effects are rate limiting during this stage.

3. During the third stage, the temperature decreases and adsorption proceeds further. For a fast-diffusing species, equilibrium adsorption occurs during this stage. As can be easily seen from Eq. A4, a temperature relaxation occurs with an exponential decay that is independent of mass diffusion. For a slow-diffusing species, nonequilibrium adsorption occurs during this stage. The rate limitation is caused by both heat effects and mass diffusion.

The curve fitting of the model depends on several thermodynamic parameters (especially $(\partial q/\partial p)_T$ and $(\partial q/\partial T)_P$), which are obtained from the equilibrium isotherm. There are also three important kinetic parameters:

- The intracrystalline diffusion coefficient
- The global heat-transfer coefficient

• The barrier for mass transfer at the crystal surface, if it exists.

The heat-transfer coefficient h that accounts for the overall heat transfer between the sample and the surroundings (including radiation, conduction through the sample holder and through the gas) is easily obtained from the zeroth moment of the surface temperature according to Eq. A6. Therefore, two mass-transfer parameters are obtained by curve fitting: the intracrystalline coefficient and the surface barrier coefficient when such a surface barrier does exist.

In the simplest case without a surface barrier, the determination of the intracrystalline diffusion coefficient is straightforward since it is the only parameter to be fitted. Figure 2 shows this phenomenon in the case of the adsorption of water on a single layer of large (100 μm) NaX crystals. In this case, the limiting process is the time needed to produce the pressure step itself, so that only a lower limit of the diffusivity can be obtained in this experiment. The value obtained by this thermal method ($D_0 = 0.6 \times 10^{-10}$ m^2·s^{-1}) is close to the value obtained by the NMR technique ($D_0 = 0.7$ to 1.4×10^{-10} m^2·s^{-1}) (Pfeifer, 1976; Pfeifer et al., 1985) in Leipzig. This shows that this is the fastest adsorption kinetics corresponding to a characteristic time equal to 0.2 s that can be measured with this equipment. The agreement is important since, in general, the agreement between NMR and uptake techniques is much less satisfactory for diffusion in NaX than in A zeolites since X-system is much faster. It has to be noted that the characteristic time due to intracrystalline mass diffusion is only 0.2 s, while the heat-transfer characteristic time is 136 s (Table 1).

NaX–CH_3OH (100-μm crystals). Following the experiments with water, a series of experiments of adsorption of methanol vapor on the same sample were performed. After the first experiment with the fresh sample, the solid was heated *in situ* under vacuum to desorb methanol. The sample was then cooled *in situ* to ambient temperature and another experiment was performed, and so on. It rapidly appeared that the kinetics of adsorption depend strongly on the sample history. Therefore, a systematic study of reproducibility was undertaken and more than 100 experiments were performed. Sequences of pressure steps (50–80 and 80–50 Pa) were imposed after regeneration at various temperatures. Analysis of the results shows that the first two experiments (before any thermal regeneration in the presence of methanol vapor) are consistent with the purely diffusive model, and the value of the diffusivity is consistent with the NMR data as well as with the ZLC data (Grenier et al., 1994). The sensitivity of the model on the value of the intracrystalline diffusivity is displayed in Figure 3a; the solid line corresponds to the identified intracrystalline diffusivity ($D_c = 0.68 \times 10^{-10}$ m^2·s^{-1}), while the dashed lines correspond to an infinite diffusivity (short dashes); the intermediate dashes correspond to $D_c = 2 \times 10^{-10}$ m^2·s^{-1} and the long dashes correspond to $D_c = 0.23 \times 10^{-10}$ m^2·s^{-1} (the values of the darken factor and of the corrected diffusivity are given in Table 2). In Figure 3b, the influence of the mass rate-limiting effect is displayed, and experimental points are compared to two theoretical curves: the solid line corresponds to a purely diffusive model, while the dashed line corresponds to a model in which the mass-transfer limitation is due to a barrier at the crystal surface.

Table 1. NaX Zeolite–H_2O Results

A. Sample and Data

Sample	Procedure Pressure	$(\partial q/\partial p)$ (kg·m^{-3}·Pa^{-1})	$(\partial q/\partial T)$ (kg·m^{-3}·K^{-1})	$(\partial \ln p/\partial \ln q)$ (Darken factor)	λ (W·m^{-1}·K)	Loading (kg·m^{-3}‡)
Crystals (100 μm) monolayer	Δp 50–80 Pa	0.72	−3.5	8	∞	400
1 mm dia. pellets monolayer	ΔV 100 Pa	0.39	−3.0	10.2	0.21†	430
Single pellet 4-mm dia.	Δp 193–140 Pa	0.21	−2.5	20.5	0.23*	450

B. Experimental Results

Sample	D_c (m^2·s^{-1})	D_0 (m^2·s^{-1})	D_p (m^2·s^{-1})	h (W·m^{-2}·s^{-1})	t_{Dc} (s)	t_{Dp} (s)	t_h (s)	t_λ (s)
Crystals	$> 5 \times 10^{-10}$	$> 6\ 10^{-11}$	—	1.8	< 0.2	0	136	0
1-mm-dia. beads	10^{-10}§	—	4.5×10^{-5}	5.3	< 0.2	23	100	0.2
4-mm-dia. pellets	10^{-10}§	—	4×10^{-5}	4.5	< 0.2	405	1,300	5.8
4-mm-dia. single pellet	10^{-10}§	—	4.5×10^{-5}	10	< 0.2	240	250	5.6

*Thermal conductivity identified from this experiment.
†Input in the numerical simulation (Sahnoune and Grenier, 1989).
‡kg·m^{-3} of crystals.
§Input in the model.

Table 2. Results on NaX–CH_3OH

A. Procedure and Data

Run	Procedure Pressure	$(\partial q/\partial p)$ $(kg\cdot m^{-3}\cdot Pa^{-1})$	$(\partial q/\partial T)$ $(kg\cdot m^{-3}\cdot K^{-1})$	$(\partial \ln p/\partial \ln q)$ (Darken factor)	Loading $(kg\cdot m^{-3})$
Figure 3	Δp 48–80 Pa	0.15	−0.9	26.3	240
Figure 4	Δp 49–79 Pa	0.08	−0.5	26.3	

B. Experimental Results

Run	D_c (m^2s^{-1})	D_0 (m^2s^{-1})	k_c $(m\cdot s^{-1})$	h $(W\cdot m^{-2}\cdot s^{-1})$	t_{mc} (s)	t_{sc} (s)	t_h (s)
Figure 3	6.8×10^{-11}	2.6×10^{-12}	∞	2.3	1.9	0	25
Figure 4	2.0×10^{-11}	7.6×10^{-13}	1.7×10^{-6}	2.3	8.2	9.8	25

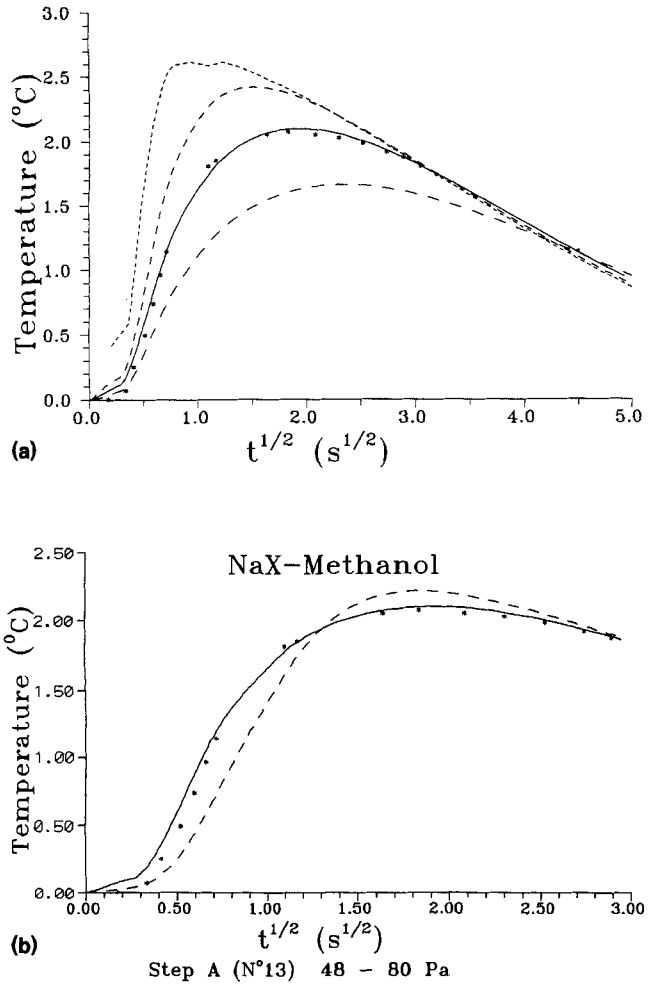

Figure 3. Temperature response of a 100-μm NaX crystals single layer after a pressure step of CH_3OH vapor on the fresh sample (48–80 Pa).

(a) The experimental results (symbols) are compared to four theoretical curves all given by a purely diffusive model (solid line, $D_c = 0.68\times10^{-10}$ $m^2\cdot s^{-1}$; short dashes, infinite diffusivity; intermediate dashes, $D_c = 2\times10^{-10}$ $m^2\cdot s^{-1}$; long dashes, $D_c = 0.23\times10^{-10}$ $m^2\cdot s^{-1}$). See Table 2. (b) The experimental results (symbols) are compared to two theoretical curves (solid line, purely diffusive model $D_c = 0.68\times10^{-10} m^2\times s^{-1}$, $R_c = 9.0\times10^{-6} m\times s^1$; dashed line, surface barrier).

The best fit is obtained with the purely diffusive model. For the subsequent experiments after thermal regeneration at 300°C under low pressure of methanol vapor (less than 0.1 Pa), a good curve fit with a purely diffusive model is no longer possible. This discrepancy is attributed to a nondiffusive transport phenomenon since the quality of the experimental results is good. This nondiffusive transport phenomenon is assumed to be a surface barrier. An extra parameter is then introduced for the curve fitting and an excellent agreement is obtained (Figure 4). The explanation that has been proposed to analyze these results is that a nonvolatile component (coke) would be formed each time the temperature is raised at 300°C in the presence of methanol (even at low pressure). This nonvolatile component formation would be responsible for the development of a surface barrier and thus for the observed decline in sorption rate. As a consequence of the combination of both effects, the mass-transfer characteristic time is enhanced by a factor of 10 (Table 2) or even 14 (Grenier et al., 1994). A detailed analysis of these results can be found in Grenier et al. (1994). These results demonstrate that, as far as adsorption of hydrocarbons is concerned, the pretreatment of the samples is a crucial factor for obtaining the true intracrystalline coefficient of diffusion of the unpolluted sample. Moreover, this also suggests that in the industrial processes involving adsorption of hydrocarbons at elevated temperatures, the kinetics of adsorption may be strongly affected by coking and that the intracrystalline coefficient of diffusion obtained on fresh samples may highly overestimate the kinetics of adsorption.

From the results on adsorption of water or methanol on NaX zeolite, it can be concluded that intracrystalline diffusion can be measured, using this thermal method, with precision even for fast-diffusing species, but this requires the measurements to be made with large crystals. If the measurements were performed on small crystals (2 μm), the response time would be divided by 2,500. In the case of the experiment with water presented on Figure 2, this leads to a characteristic time equal to 10^{-4} s, which would be far beyond the performances of the equipment. The diffusion of methanol, although slower, could not be measured either, since the characteristic time would be equal to 10^{-3} s, which is still beyond the performances of the equipment.

As shown in Figures 2 and 3, all the information required to obtain the diffusion coefficient is contained in the first

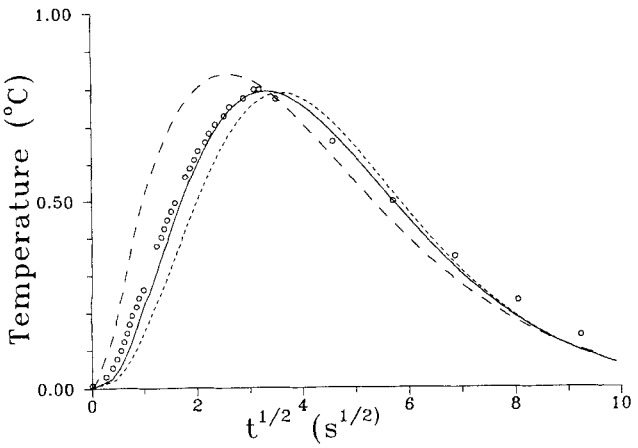

Figure 4. Temperature response of the same 100-μm NaX crystals single layer, as in Figure 3, after a pressure step of CH_3OH vapor (49–79 Pa) on the sample after thermal regeneration under the presence of methanol vapor at low pressure.

The experimental results (symbols) are compared to three theoretical curves (solid line, best fit with a model including mass diffusion $D_0 = 7.6 \times 10^{-13}$ m^2·s^{-1}, and surface barrier $k_c = 1.7 \times 10^{-6}$ ms^{-1}; short dashes, purely diffusive model $D_0 = 3.4 \times 10^{-13}$ m^2·s^{-1}; long dashes, surface barrier only $k_c = 0.9 \times 10^{-6}$ ms^{-1}). In all cases, the mass-transfer characteristic time is set equal to 18 s.

second after the pressure step for fast-diffusing species. This dictates severe requirements on the precision of the experimental setup. As depicted in Figure 4, the quality of the temperature measurement associated with the detailed model makes it possible to discriminate between intracrystalline effects and surface effects; this should be important in detailed studies of aging or coking effects.

Pellets

The extraction of the intracrystalline diffusion coefficient on standard industrial pellets consisting of agglomerated small

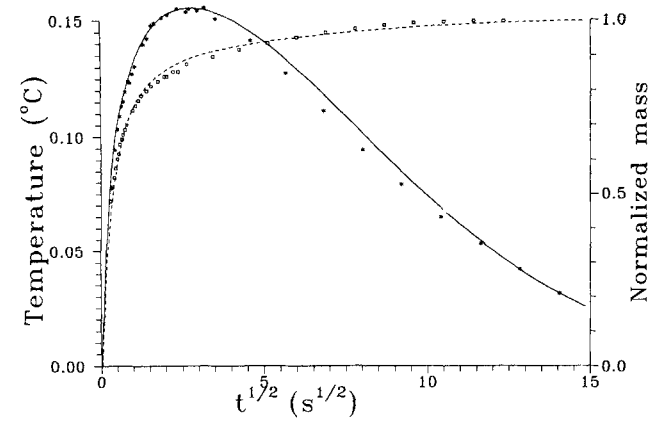

Figure 5. Temperature and mass responses of 1-mm-dia. spherical NaX pellets after a volume step ($K = 0.94$) of H_2O vapor at 113 Pa.

The experimental results (open symbols, mass; stars, temperature) are compared to theoretical curves (see Table 1).

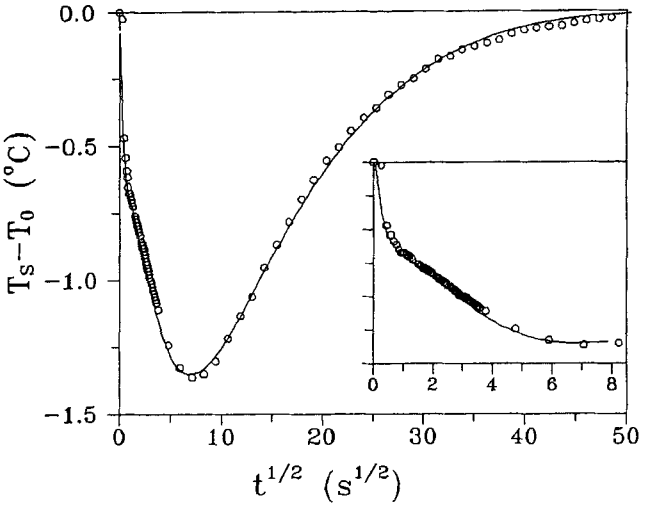

Figure 6. Temperature response of a single 4-mm dia. spherical pellet of NaX zeolite after a negative pressure step of H_2O vapor (193–140 Pa).

Experimental results (circles) are compared to the theoretical curve (see Table 1).

crystals in a binder is much more complicated since several mass-transfer limitations may exist. This requires a rigorous experimental procedure in order to discriminate between the various rate-limiting effects:

- Heat effects.
- Crystal scale effects: diffusion (micropore diffusion) as well as possible surface barriers.
- Pellet scale effects: diffusion (macropore diffusion) as well as possible surface barriers.

As the samples consist of pellet monolayers, there is no mass-transfer limitation at the bed scale. With two specific examples, it will now be shown that reliable information can be drawn from experiments when a rigorous experimental procedure is followed.

To discriminate between crystal scale and pellet scale effects, it is recommended (Ruthen, 1984) to perform measurements on several pellet sizes. The influence of pellet size is displayed in Figures 5 to 8 for two systems: NaX–water (Figures 5–7) and zeolon–methanol (Figure 8). The difference between the two systems is demonstrative:

- In the case of NaX–water, the comparison of the experimental results obtained on 1-mm- and 4-mm-dia. spheres shows that the characteristic time depends strongly on particle size (the maximum temperature variation is observed at $t^{1/2} \sim 3$ s$^{1/2}$ and 13 s$^{1/2}$ for 1-mm and 4-mm beads, respectively),
- Conversely, in the case of zeolon methanol, the response time is roughly the same for large and small pellets ($t^{1/2} \sim 11$ s$^{1/2}$).

This proves that pellet scale effects are rate limiting for NaX–water, while for zeolon–methanol, pellet scale effects are negligible and crystal effects are rate limiting. As crystal effects are rate limiting in the case of zeolon–methanol, the

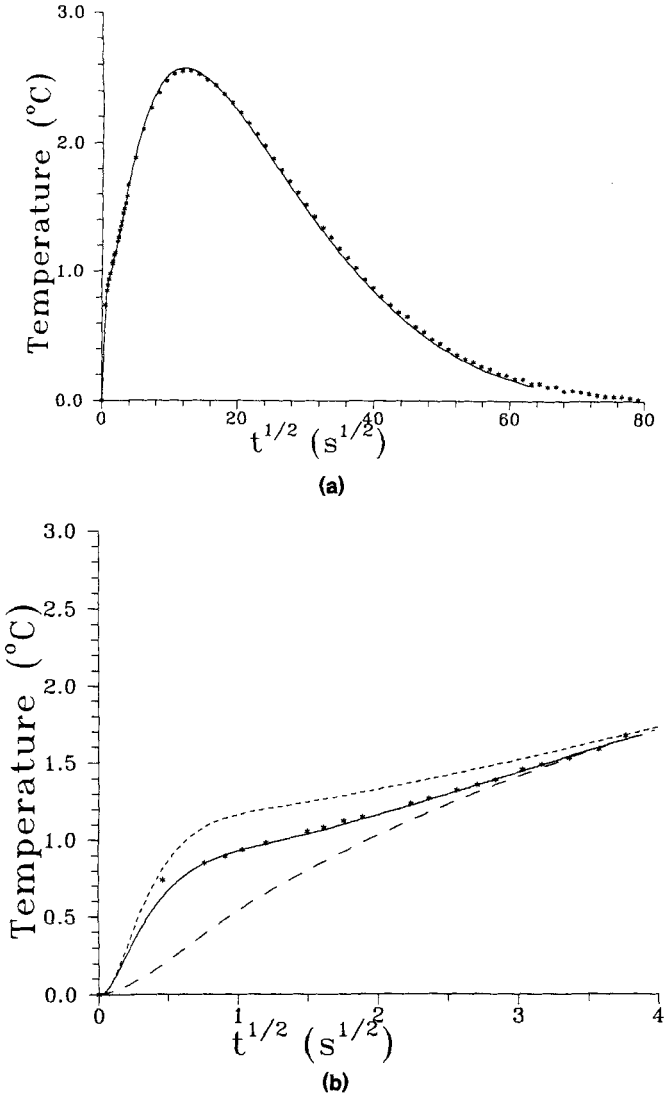

Figure 7. Temperature response of 4-mm dia. spherical pellets of NaX zeolite after a pressure step of H_2O vapor (115–154 Pa).

(a) Experimental measurements (symbols) and best theoretical fit (solid line). (b) Experimental results (symbols) are compared to three theoretical curves to display the influence of the pellet thermal conductivity (full line: $\lambda = 0.23$ $W \cdot m^{-1} \cdot K^{-1}$; dotted lines: short dash, $\lambda = 0.1$ $W \cdot m^{-1} \cdot K^{-1}$ and long dash, $\lambda = \infty$).

intracrystalline diffusion coefficient can be extracted from the experiments with pellets.

Diffusion of Methanol in Zeolon Pellets. Zeolon is a mordenite of type 900 H synthesized by Norton that has a unidimensional channel structure. Uptake rates of methanol have been measured with a small sample of zeolon cylindrical binderless pellets of crystals 9 μm long and 2 μm dia. The response of 0.5- and 1.6-mm-dia. pellets is shown in Figure 8 and the data are summarized in Table 3. The best fit on the 0.5-mm-dia. and 1.6-mm pellets gives slightly different values of 6×10^{-15} and 9×10^{-15} $m^2 \cdot s^{-1}$, respectively, for the corrected intracrystalline diffusion coefficient. The overall uptake rate is essentially controlled by the heat exchange (Table 3).

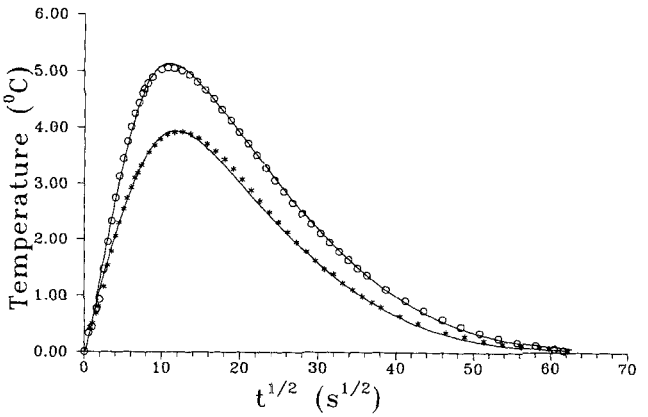

Figure 8. Temperature responses of 0.5- and 1.6-mm-dia. pellets of mordenite 900H after a pressure step of CH_3OH vapor (130–460 Pa.).

Theoretical curves are superimposed on experimental points (open circles, extrudates; stars, crushed pellets). See Table 3.

Diffusion of Water in NaX-Zeolite Pellets. The NaX pellets studied here are commercial pellets prepared by CECA. They consist in an agglomeration of crystals about 2 μm dia. with a clay binder (about 20%). A volume step experiment is performed with the 1-mm pellets experiment when pressure-step experiments are performed with the 4-mm pellets. Furthermore, measurements were performed on a single pellet (a negative pressure step experiment is shown in Figure 6). With the volume step experiment, the temperature and the mass are determined independently, whereas only the temperature can be used to measure the kinetics with the pressure step experiment. The response time is different for the two first experiments, which points out the role of pellet scale size as pointed out earlier.

Volume-step experiments have been performed with monolayers of NaX beads of 1 mm dia. The temperature is, as previously, directly obtained from the IR detector. The mass is obtained from the pressure measurement assuming an isothermal ideal gas behavior after calibration of the volume. The heat-transfer coefficient h is obtained from the zeroth moment of temperature response; the pellet thermal conductivity λ is set equal to 0.21 (Sahnoune and Grenier, 1989). D_c is taken equal to 0.6×10^{-10} $m^2 \cdot s^{-1}$ as obtained earlier from the measurements on the crystals, and D_p is obtained by curve fitting. As can be seen from Figure 5, excellent agreement between the model and experimental results is obtained for both the temperature and the mass variation. Figure 7 shows the evolution of the surface temperature of 4-mm-dia. pellets after a pressure step. The influence of the pellet thermal conductivity is clearly displayed (Figure 7b) since the uniform temperature model ($\lambda = \infty$) is unable to describe the observed shoulder at the very beginning of the pressure step; the outside layer of crystals heats up much faster than the thermal dissipation in the pellet. Conversely, the nonisothermal model used with a finite pellet thermal conductivity fits the experimental points well as soon as a correct value for the thermal conductivity is chosen. It is therefore possible to determine the thermal conductivity of the pellets with this technique. This experimental effect is obviously the consequence of the technique used here: pellet

Table 3. Zeolon-Methanol Results

A. Procedure Data

Sample	Procedure Pressure	$(\partial q/\partial p)$ $(kg\cdot m^{-3}\cdot Pa^{-1})$	$(\partial q/\partial T)$ $(kg\cdot m^{-3}\cdot K^{-1})$	$(\partial \ln p/\partial \ln q)$ (Darken factor)	λ $(W\cdot m^{-1}\cdot K)$	Loading $(kg\cdot m^{-3\dagger})$
Crystals pellets (0.5 mm)	Δp 130–460 Pa	0.018	−0.30	20	0.2*	95
Extrudates (1.6 mm)	Δp 130–460 Pa	0.018	−0.30	20	0.2*	95

B. Experimental Results

Sample	D_c $(m^2\cdot s^{-1})$	D_0 $(m^2\cdot s^{-1})$	D_p $(m^2\cdot s^{-1})$	h $(W\cdot m^{-2}\cdot s^{-1})$	t_{Dc} (s)	t_{Dp} (s)	t_h (s)	t_λ (s)
Crushed pellets (0.5 mm)	1.1×10^{-13}	0.6×10^{-14}	2×10^{-5}	0.17	63	0.70	860	4.6
Extrudates (1.6 mm)	1.7×10^{-13}	0.9×10^{-14}	2×10^{-5}	0.53	41	11	980	4.6

*Input in the numerical simulation.
†$kg\cdot m^{-3}$ of crystals.

surface temperature measurement rather than pellet bulk temperature.

Experiments on a single pellet have also been performed. A specific arrangement has been built in which a single pellet is placed in a gold-plated cone with the optics of the IR detector adjusted to focus on the single-pellet surface. The surface temperature variation (Figure 6) is characterized by two distinct breaks, indicating that the kinetics are limited by at least three different transport processes. As pointed out earlier, the extremely rapid initial change of the surface temperature is a result of very fast intracrystalline diffusion and the first break is essentially caused by a finite-rate of heat conduction through the pellet. From this experiment, only a lower limit can be established for the intracrystalline diffusivity: $D_0 > 5\times10^{-14}$ $m^2\cdot s^{-1}$ ($t_{D_c} < 0.2$ s). As discussed before, the exact shape of the curve depends on the pellet thermal conductivity, the derived value of the pellet thermal conductivity λ is 0.23 $W\cdot m^{-1}\cdot s^{-1}$ ($t_\lambda = 5.6$ s) close to the previous measurements (Sahnoune and Grenier, 1989). The second break is due to the competition between the macropore diffusion and heat exchange at the pellet surface.

As the overall kinetics are not sensitive to the intracrystalline diffusion, no precise information on this intracrystalline diffusion can be extracted from these experiments on pellets. Nevertheless, these experiments give very precise information on the global mass-transfer characteristic time as well as on the macropore coefficient of diffusion and on the linear driving force (LDF) coefficient for this system (Glueckauf and Coates, 1947):

$$\frac{\partial q}{\partial t} = k(q^x - q) \tag{3}$$

where q^x is the equilibrium sorbate concentration and k is the LDF coefficient related to the global mass-transfer characteristic time:

$$\frac{1}{k} = t_{S_c} + t_{D_c} + t_{S_p} + t_{D_p} \tag{4}$$

The mass-transfer characteristic time in Eq. 4 is the global mass-transfer characteristic time obtained directly from the experiment on pellets, and it is the information required for most of column dynamics work. This mass-transfer characteristic time is related to the detailed mass-transfer characteristic times through Eq. A16 (Sun, 1988).

The precise data obtained from the analysis of the experimental results using a bidisperse nonisothermal model are presented in Table 1. The summarized experimental results obtained for the NaX–water system with three different samples (large crystals and two different pellets size) yield coherent data. This proves that the intracrystalline diffusivity is very fast and that macropore diffusion is rate limiting for pellets. Macropore diffusivity close to 4.5×10^{-5} $m^2\cdot s^{-1}$ is obtained that corresponds to a macropore diffusion in the Knudsen regime.

Now, with respect to heat-transfer effects:

- The characteristic time due to thermal conductivity is completely negligible for the crystals. The Lewis number, $Le = 3{,}300$, is much higher than 10, which is the condition for a uniform temperature model to be valid (Sun and Meunier, 1987b) and a uniform temperature model has been used. For the pellet, the characteristic time due to the pellet thermal conductivity is small but, in general, it is no longer negligible and a uniform temperature model must be used. The analysis of the results of the numerical simulation for the 1-mm pellets (Table 1) shows that the characteristic time corresponding to the thermal conductivity in the crystal is small (0.2 s) because the pellet size is small; therefore, the curve as obtained from the model is not very sensitive to the pellet thermal conductivity, and a uniform temperature model would be convenient as well. In contrast, the numerical simulation for the 4-mm pellet is sensitive to the value of the pellet thermal conductivity and the value that has been identified (0.23 W·

$m^{-1}\cdot s^{-1}$) is in good agreement with direct measurements (Sahnoune and Grenier, 1989).

• The characteristic time for the heat exchange between the sample and the environment is in all cases very high (between 100 and 250 s). The heat exchange coefficient, h, is very low and varies highly depending on the experimental procedure (from 1.8 to 10 $W\cdot m^{-2}\cdot s^{-1}$). The overall heat transfer for the whole sample does not vary much from one experiment to another. Conversely, the heat-transfer coefficient h per crystal (or pellet) m^2 depends strongly on the sample geometry.

Limits of the method

The method is obviously limited for very-fast-diffusing species, but it is also limited for slow-diffusing species. The limit for the fast-diffusing species comes from the overall response time of the equipment, which is about 0.2 s for the pressure step, mainly due to the time for pressure variation. This means that if the characteristic time is less than 0.2 s, it cannot be detected by the pressure step technique. This characteristic time $t_{D_c} = 0.2$ s dictates the upper value of the diffusivity that can be measured with the pressure step thermal method, which corresponds to $D_c = 5\times10^{-10}$ $m^2\cdot s^{-1}$ for 100-μm-dia. spherical crystals and $D_c = 5\times10^{-14}$ $m^2\cdot s^{-1}$ for 1-μm-dia. crystals. With respect to the corrected diffusivity, the limit depends on the darken factor. It has been shown to be $D_0 < 0.6\times10^{-10}$ $m^2\cdot s^{-1}$ for 100-μm crystals when the Darken factor equals 8. For industrial pellets, assuming the same Darken factor and a 2-μm-dia. crystal size, the limit on D_0 would be less than 2.5×10^{-14} $m^2\cdot s^{-1}$. This is why the intracrystalline diffusivity could be measured with the zeolon-methanol system with relatively small crystals (9 μm long) aggregated in pellets. The diffusivities were found to be 1.1×10^{-13} $m^2\cdot s^{-1} < D_c < 1.7\times10^{-13}$ $m^2\cdot s^{-1}$ and 6×10^{-15} $m^2\cdot s^{-1} < D_0 < 9\times10^{-15}$ $m^2\cdot s^{-1}$. With the volume step, the response is faster by a factor of 10 (characteristic time $\sim$ 20 ms). Diffusivities as high as $D_c \sim 5\times10^{-9}$ $m^2\cdot s^{-1}$ and corrected diffusivities $D_0 \sim 10^{-10}$ $m^2\cdot s^{-1}$ can be measured with precision for 100-μm spherical crystals.

The limit of the thermal method for the slow-diffusing species comes from the sensitivity of the IR temperature measurement. If the kinetics of adsorption is very slow, the temperature variation is also very small and it can be too small to be measured. It is estimated that the diffusivity D_c should be higher than 10^{-16} $m^2\cdot s^{-1}$, with small crystals, to be measured with precision. This corresponds to corrected diffusivities in the range of 10^{-17} $m^2\cdot s^{-1}$, depending on the Darken factor. The range for diffusivity measurement with the volume step equipment is of the order of 10^{-15} $m^2\cdot s^{-1} < D_c < 10^{-8}$ $m^2\cdot s^{-1}$ (10^{-17} $m^2\cdot s^{-1} < D_0 < 5\times10^{-10}$ $m^2\cdot s^{-1}$).

Conclusion

Experimental results obtained on zeolite crystals as well as on zeolite pellets demonstrate the feasibility of a thermal method based on the measurement of sample surface temperature via the IR emission to determine the coefficients of mass diffusion.

Pressure-step experiments performed on crystals prove that the intracrystalline mass diffusion can be extracted with good precision if the crystal size is large enough. The faster the intracrystalline diffusion, the larger the required crystal size. For instance, with 100-μm NaX crystals, it is possible to determine an intracrystalline diffusivity D_c as high as 5×10^{-10} $m^2\cdot s^{-1}$ (corresponding to a corrected diffusivity D_0 as high as 0.6×10^{-10} $m^2\cdot s^{-1}$) for H_2O. With the same 100-μm NaX crystals, moderate values of the corrected intracrystalline diffusivity of 2.6×10^{-12} $m^2\cdot s^{-1}$ for CH_3OH can be determined with high precision. For small industrial crystals (2 μm), it is not possible to extract the intracrystalline coefficient of diffusion for fast-diffusing species. This may explain why, in the literature, the agreement between NMR and uptake techniques is much less satisfactory for diffusion in NaX than in A zeolites. The lack of precision of most uptake techniques for fast-diffusing species may be an explanation. Therefore, the good agreement reported on the results presented herein with NMR measurements (for NaX–H_2O) (Pfeifer, 1976; Förste et al., 1989) and with NMR as well as with ZLC (NaX–CH_3OH) (Grenier et al., 1994) is important since it demonstrates the reliability of the technique for fast-diffusing species when large crystals are used. The high sensitivity of the experimental technique combined with a detailed model (Sun and Meunier, 1987a) allows discrimination between intracrystalline and surface effects. In the NaX–CH_3OH experiments, a nondiffusive effect was observed in some experiments. This was attributed to the appearance of a surface barrier that could be due to coke formation after thermal regeneration in the presence of methanol vapor. This thermal method seems to be a useful tool to investigate the evolution of surface barriers according to aging when hydrocarbons are used at elevated temperatures.

Experiments performed on pellets clearly show that in all cases the effective characteristic time for mass transfer can be extracted with a good precision. This is important since the characteristic time yields an LDF coefficient useful for column dynamics modeling. However, in the case of pellets, the intracrystalline diffusivity can be extracted with reasonable precision only for slow diffusing species and it requires a rigorous experimental procedure using different pellet sizes. When the intracrystalline diffusion characteristic time is greater than 0.2 s, the intracrystalline diffusivity can be extracted with a reasonable precision from pressure-step measurements on pellets. This has been shown for the mordenite H (zeolon)–CH_3OH system, which is a slow diffusing system. With a volume step technique, the characteristic time limit is lowered to about 0.02 s, but it is still too high to allow the extraction of the intracrystalline diffusivity from pellets for the NaX–H_2O system, since the crystal size is too small. In the case of large pellets (4 mm dia.), it is shown that the pellet thermal conductivity is an important parameter for the response of the measured pellet surface temperature.

The experimental technique described herein could be used for adsorbents other than zeolite (active carbon, silica gel, alumina, and so on), but the model used would have to be adapted to the physical process governing the kinetics of adsorption in these other adsorbents.

Acknowledgments

The support of this work through a contract from the CEC (Joule program) is gratefully acknowledged. The authors want to thank N. Coron, G. Dambier, and J. Leblanc from IAS-CNRS for their important contribution in achieving the high-sensitivity IR detection de-

vice. The NaX crystals were kindly provided by Professor S. P. Zhdanov via Professor J. Kärger. Discussions with Professor D. M. Ruthven during this work were highly appreciated.

Literature Cited

Barrer, R. M., and D. W. Brook, "Molecular Diffusion in Chabazite, Mordenite and Levynite," *Trans. Farad. Soc.*, **49**, 1049 (1953).

Beschmann, K., S. Fuchs, and L. Riekert, "Kinetics of Sorption of Benzene and *n*-Paraffins in Large Crystals of MFI Zeolites," *Zeolites*, **10**, 798 (1990).

Chiang, A. S., A. G. Dixon, and Y. H. Ma, "The Determination of Zeolite Crystal Diffusivity by Gas Chromatography: II Experimental," *Chem. Eng. Sci.*, **39**, 1461 (1984).

Eic, M., and D. M. Ruthven, "A New Experimental Technique for Measurement of Intracrystalline Diffusivity," *Zeolites*, **8**, 40 (1988).

Förstë, Chr., A. Germmanus, J. Kärger, G. Mobius, M. Bälon, S. P. Zhdanov, and N. N. Teoklistora, "Tuisotz von Deuterierten Molekülеuzur Bestimmung," *Isotopeupiaxis*, **23**(2), 48 (1989).

Glueckauf, E., and J. L. Coates, "Theory of Chromatography. Part IV. The Influence of Incomplete Equilibrium on the Front Boundary of Chromatograms and on the Effectiveness of Separation," *J. Chem. Soc.*, 1315 (1947).

Grenier, Ph., F. Meunier, J. Kärger, Z. Xu, and D. M. Ruthven, "Diffusion of Methanol in NaX Crystals: Comparison of IR, ZLC and NMR PFG Measurements," *Zeolite*, **14**, 242 (1994).

Hayhurst, D. T., and A. R. Paravar, "Diffusion of C1 to C5 Normal Paraffins in Silicalite," *Zeolites*, **8**, 27 (1988).

Jobic, H., M. Bée, and G. J. Kearley, "Translational and Rotational Dynamics of Methane in ZSM-5 Zeolite: A Quasi-elastic Neutron Scattering Study," *Zeolites*, **9**, 312 (1989).

June, R. L., A. T. Bell, and D. N. Theodorou, *Mol. Simulation*, **8**, 73 (1991).

Karge, H., and W. Niessen, *Catal. Today*, **8**, 451 (1991).

Kärger, J., and D. M. Ruthven, *Diffusion in Zeolites*, Wiley, New York (1992).

Kärger, J., and D. M. Ruthven, "On the Comparison between Macroscopic and n.m.r. Measurements of Intracrystalline Diffusion in Zeolites," *Zeolites*, **9**, 267 (1989).

Maginn, E. J., A. T. Bell, and D. N. Theodorou, "Prediction of the Transport Diffusivity of Methane in Silicalite Using Equilibrium and Nonequilibrium Simulation Techniques," AIChE meeting, Miami (Nov. 2–6, 1992).

Pfeifer, H., "Surface Phenomena Investigated by Nuclear Magnetic Resonance," *Phys. Rep.*, **26**, 29 (1976).

Pfeifer, H., J. Kärger, A. Germanus, W. Schirner, M. Bülow, and J. Caro, "Concentration Dependence of Intracrystalline Self-Diffusion in Zeolites," *Adsorption Sci. Tech.*, **2**, 229 (1985).

Ruthven, D. M., and R. Kumar, "An Experimental Study of Single-Component and Binary Adsorption Equilibria by a Chromatographic Method," *Ind. Eng. Chem. Fundam.*, **19**, 27 (1980).

Ruthven, D. M., *Principles of Adsorption and Adsorption Processes*, Wiley-Interscience, New York (1984).

Sahnoune, H., and Ph. Grenier, "Mesure de la Conductivité Thermique d'une Zéolithe," *Chem. Eng. J.*, **40**, 45 (1989).

Schneider, P., and J. M. Smith, "Adsorption Rate Constants from Chromatography," *AIChE J.*, **14**, 762 (1968).

Smivoc, R. Q., R. I. June, A. I. Bell, and D. N. Theodorou, "Molecular Simulations of Methane Adsorption in Silicalite," *Mol Simulation*, **8**, 3 (1991).

Sun, L. M., and F. Meunier, "Non-isothermal Adsorption in a Bidisperse Adsorbent Pellet," *Chem. Eng. Sci.*, **42**, 2899 (1987a).

Sun, L. M., and F. Meunier, "A Detailed Model for Non-isothermal Sorption in Porous Adsorbents," *Chem. Eng. Sci.*, **42**, 1585 (1987b).

Sun, L. M., "Contribution à la Cinétique d'Adsorption de Gaz," PhD Thesis, Paris 6 (1988).

Torresan, A., and Ph. Grenier, "Un Appareil pour la Mesure thermique de la Cinétique d'Adsorption," *Chem. Eng. J.*, **49**, 11 (1992).

Van den Begin, N. G., and L. V. C. Rees, "Diffusion of Hydrocarbons in Silicalite using a Frequency Response Method," *Zeolites, Facts, Figures, Future*, Elsevier, Amsterdam, p. 915 (1989).

Yasuda, Y., Y. Suzuki, and H. Fukada, "Kinetic Details of a Gas/Porous Adsorbent System by the Frequency Response Method," *J. Phys. Chem.*, **95**, 2486 (1991).

Zhong, G. M., Ph. Grenier, and F. Meunier, "Influence des Transferts Intergranulaires sur la Détermination Gravimétrique de la Cinétique d'Adsorption," *Chem. Eng. J.*, **33**, 147 (1993).

Appendix

Diffusion model for a crystal

The mass balance in the crystal:

$$\frac{\partial q}{\partial t} = \frac{D_c}{r_c^\sigma}\frac{\partial}{\partial r_c}\left(r_c^\sigma \frac{\partial q}{\partial r_c}\right) \tag{A1}$$

$$\left.\frac{\partial q}{\partial r_c}\right|_{r_c=0} = 0 - D_c \left.\frac{\partial q}{\partial r_c}\right|_{r_c=R_c} = k_c(q|_{r_c=R_c} - q^*), \tag{A2}$$

where σ is the geometrical factor for the crystal (= 0, 1, 2 for a slab, cylinder, and sphere, respectively). The mass adsorbed at equilibrium is given by

$$q^* - q_0 = K_p(P - P_0) - K_T(T - T_0). \tag{A3}$$

The heat balance

$$C_S\frac{dT}{dt} = \frac{(\sigma+1)h}{R_c}(T_0 - T) + |\Delta H|\frac{\partial \bar{q}}{\partial t}. \tag{A4}$$

The mass conservation in the chamber

$$\frac{PV_e}{RT_0} + V_s\bar{q} = \text{constant}. \tag{A5}$$

The zeroth moment of the temperature is given by

$$\int_0^\infty (T - T_0)\quad dt = \frac{R_c|\Delta H|(q_\infty - q_0)}{(\sigma+1)h}. \tag{A6}$$

The ratio between the first and zeroth moments of the temperature is

$$\frac{\int_0^\infty (T - T_0)t\quad dt}{\int_0^\infty (T - T_0)\quad dt} = \frac{1}{1+K}(t_{S_c} + t_{D_c} + t_h) \tag{A7}$$

with

$$K = \frac{V_s K_p R T_0}{V_e}$$

$$t_{D_c} = \frac{R_c^2}{(\sigma+1)(\sigma+3)D_c} \qquad t_{S_c} = \frac{R_c}{(\sigma+1)k_c}$$

$$t_h = (C_S + |\Delta H|K_T)\frac{R_c}{(\sigma+1)h}$$

Diffusion model for a pellet

The diffusion equations for the pellet and crystals:

$$\frac{\partial c_p}{\partial t}+\frac{1-\epsilon}{\epsilon}\frac{\partial \bar{q}}{\partial t}=\frac{D_p}{r_p^{\nu}}\frac{\partial}{\partial r_p}\left(r_p^{\nu}\frac{\partial c_p}{\partial r_p}\right) \tag{A8}$$

$$C_S\frac{\partial T}{\partial t}-(1-\epsilon)|\Delta H|\frac{\partial \bar{q}}{\partial t}=\frac{\lambda}{r_p^{\nu}}\frac{\partial}{\partial r_p}\left(r_p^{\nu}\frac{\partial T}{\partial r_p}\right) \tag{A9}$$

$$\frac{\partial q}{\partial t}=\frac{D_c}{r_c^{\sigma}}\frac{\partial}{\partial r_c}\left(r_c^{\sigma}\frac{\partial q}{\partial r_c}\right), \tag{A10}$$

where ν is the geometrical factor for the pellet.

The corresponding boundary conditions are

$$\left.\frac{\partial c_p}{\partial r_p}\right|_{r_p=0}=0 \qquad -D_p\left.\frac{\partial c_p}{\partial r_p}\right|_{r_p=R_p}=k_p(c_p|_{r_p=R_p}-c_g) \tag{A11}$$

$$\left.\frac{\partial T}{\partial r_p}\right|_{r_p=0}=0 \qquad -\lambda\left.\frac{\partial T}{\partial r_p}\right|_{r_p=R_p}=h(T|_{r_p=R_p}-T_0) \tag{A12}$$

$$\left.\frac{\partial q}{\partial r_c}\right|_{r_c=0}=0 \qquad -D_c\left.\frac{\partial q}{\partial r_c}\right|_{r_c=R_c}=k_c(q|_{r_c=R_c}-q^*). \tag{A13}$$

The quantity adsorbed at equilibrium is

$$q^*-q_0=K_C(c_p-c_0)-K_T'(T-T_0). \tag{A14}$$

The mass conservation in the chamber leads to

$$V_e c_g+V_s\left[\epsilon\bar{c}_p+(1-\epsilon)\bar{\bar{q}}\right]=\text{constant}. \tag{15}$$

The ratio between the first and zeroth moment of the surface temperature, T_s, is

$$\frac{\int_0^{\infty}(T_s-T_0)t\ \ dt}{\int_0^{\infty}(T_s-T_0)\ \ dt}=\frac{1}{1+K}(t_{S_c}+t_{D_c}+t_{S_p}+t_{D_p}+t_h+t_\lambda), \tag{A16}$$

where

$$t_{D_c}=(1+\gamma)\frac{R_c^2}{(\sigma+1)(\sigma+3)D_c} \qquad t_{S_c}=(1+\gamma)\frac{R_c}{(\sigma+1)k_c}$$

$$t_{D_p}=(1+\beta)\frac{R_p^2}{(\nu+1)(\nu+3)D_p} \qquad t_{S_p}=(1+\beta)\frac{R_p}{(\nu+1)k_p}$$

$$t_\lambda=[1+K+\delta(1+\gamma)]\frac{R_p^2C_S}{(\nu+1)(\nu+3)\lambda}$$

$$t_h=[1+K+\delta(1+\gamma)]\frac{R_pC_S}{(\nu+1)h}.$$

The dimensionless thermodynamic parameters are defined by

$$K=\frac{V_s}{V_e}[\epsilon+(1-\epsilon)K_C] \qquad \delta=\frac{(1-\epsilon)|\Delta H|}{C_S}\left(K_T'-K_C\frac{P_0}{RT_0^2}\right)$$

$$\beta=\frac{1-\epsilon}{\epsilon}K_C \qquad \gamma=\frac{\epsilon V_s}{V_e}.$$

Manuscript received July 11, 1994, and revision received Oct. 19, 1994.